Remote Sensing Applications: Society and Environment 36 (2024) 101286

Contents lists available at ScienceDirect

Remote Sensing Applications: Society and Environment

journal homepage: www.elsevier.com/locate/rsase

Increasing risk of glacial lake outburst flood in Sikkim, Eastern Himalaya under climate warming

Saurabh Kaushik [a, b, *], Mohammd Rafiq [c], Jaydeo K. Dharpure [b], Ian Howat [b, d], Joachim Moortgat [b, d], P.K. Joshi [e, f], Tejpal Singh [g], Andreas J. Dietz [h]

[a] Academy of Scientific and Innovative Research (AcSIR), Ghaziabad, 201002, India
[b] Byrd Polar and Climate Research Center, The Ohio State University, Columbus, 43210, OH, USA
[c] Ministry of Environment Forest and Climate Change, New Delhi, 110003, India
[d] School of Earth Sciences, The Ohio State University, Columbus, 43210, OH, USA
[e] School of Environmental Sciences, Jawaharlal Nehru University, New Delhi, 110067, India
[f] Special Centre for Disaster Research, Jawaharlal Nehru University, New Delhi, 110067, India
[g] CSIR-Central Scientific Instrument Organisation, Chandigarh, 160030, India
[h] German Remote Sensing Data Center (DFD), German Aerospace Center (DLR), Muenchener Sr. 20, 82234, Wessling, Germany

ARTICLE INFO

Keywords:
Sikkim Himalaya
GLOF modelling
AHP
Remote sensing

ABSTRACT

The increasing risk of Glacial Lake Outburst Floods (GLOFs) in the Eastern Himalaya is exacerbated by climate change-driven glacial ice mass loss, slowdown, and increasing infrastructure projects in the high-altitude regions. To quantify the current risk of potential future disasters we update the inventory of glacial lakes in Sikkim Himalaya, identify the most potentially dangerous glacial lakes (PDGL) and model their peak discharge in different scenarios. The updated glacial lake inventory includes 232 glacial lakes (of >0.01 km^2) covering a cumulative area of 22.23 ± 0.10 km^2. Our GLOF susceptibility mapping of all moraine-dammed glacial lakes using an Analytic Hierarchy Process (AHP) reveals one lake as very high risk, eight as high risk, 22 as medium risk, 56 as low risk, and 18 as very low risk. Further, we apply dam break flood simulations for the seven most dangerous lakes. Results reveal highest peak discharges of 9504 m^3 s^{-1} and 8421 m^3 s^{-1} in extreme case scenarios from the Khanchung and South Lhonak lakes, respectively. The lowest peak discharge of 622 m^3 s^{-1} is estimated in a normal outburst event for Yongdi lake, with every scenario at least 447 m^3 s^{-1} discharge is reaching to Chungthang town. We find that more than 10,000 people face direct threat of GLOF with potential large-scale infrastructure damage (~1900 settlement, 5 bridges and 2 hydropower plants). The updated glacial lake dataset, GLOF susceptibility mapping, and modeling results demonstrate the urgent need to install an early warning system and control breaching of highly dangerous lakes.

1. Introduction

Direct impacts of global climate change are evident from glacier ice mass loss (Hugonnet et al., 2021; Lee et al., 2021; Maurer et al., 2019), slowing of ice flow due to thinning (Dehecq et al., 2019; Kaushik et al., 2022), formation of glacial lakes in high mountainous regions (Zheng et al., 2021). High Mountain Asia (HMA) is experiencing a comparatively faster rate of warming (Lalande et al., 2021) and concomitant glacier ice mass loss (Brun et al., 2017; Maurer et al., 2019). Retreating glaciers expose topographic depres-

* Corresponding author. Academy of Scientific and Innovative Research (AcSIR), Ghaziabad, 201002, India.
E-mail address: kaushik.67@osu.edu (S. Kaushik).

https://doi.org/10.1016/j.rsase.2024.101286
Received 28 February 2024; Received in revised form 11 June 2024; Accepted 30 June 2024
Available online 1 July 2024

sions that form proglacial lakes dammed by ice above and moraines, which may be ice cored, below (Kaushik et al., 2020; Song et al., 2017). Lake sizes may increase over time due to continued ice retreat, filling and coalescence with neighboring lakes. Thus, over the past two decades, there has been a noticeable increase in the size of existing proglacial lakes and the creation of new lakes in mountain ranges worldwide (Veh et al., 2020a; Zheng et al., 2021). Glacial lakes have received increasing scientific attention in the last two decades due to their relationship with glacier and Glacial Lake Outburst Flood (GLOF) hazards (Taylor et al., 2023; Veh et al., 2020a; Zheng et al., 2021). The presence of glacial lakes can also significantly alter the rate of glacier ice mass loss via calving (Pronk et al., 2021; Thakuri et al., 2016). Moreover, several studies highlight the importance of these glacial lakes to water resources (Dan H. Shugar et al., 2020). Among these factors, glacial lakes bear great significance in terms of GLOF, owing to its high carrying capabilities which can cause destruction and threat to lives in their flow path (Kaushik et al., 2020; Zheng et al., 2021). However, predicting GLOF events is complicated by the complex interaction of surface dynamics (e.g. mass movement, rockfall, landslide and seismic activity), moraine dam characteristics (e.g. dam type, height-width ratio) and hydrometeorological factors (i.e., heavy precipitation, avalanches) (Simon Keith Allen et al., 2019; Huggel et al., 2004; Kaushik et al., 2020; Worni et al., 2013). Thus, mapping and modeling potential GLOF events remain an active field of research (Dan H. Shugar et al., 2020; Taylor et al., 2023; Zheng et al., 2021).

GLOF events may result in downstream damage to infrastructure, and property as well as extensive loss of life (Aggarwal et al., 2017; Huggel et al., 2004; Kaushik et al., 2020; Sattar et al., 2019). Several recent studies have made significant progress in the assessment of the anticipated risks of GLOF hazards at regional (Veh et al., 2020a; Zheng et al., 2021) and global scales (Dan H. Shugar et al., 2020; Taylor et al., 2023). Taylor et al. (2023) quantified GLOF hazards on a global scale, revealing that 15 million people are at risk of GLOFs. They found that the HMA region is the most hazardous, with approximately 1 million people living within 10 km buffer zone of glacial lakes. Zheng et al. (2021) describes the past, present and predicted GLOF risk in the HMA. Overall, the glacial lakes has increased in number and area by 6.8 $\pm$ 0.1% and 5.9%, respectively, in the HMA between 1990 and 2015 (Zheng et al., 2021). They find that the highest risk of GLOF is in the Eastern Himalaya compared to adjacent regions. Similarly, Veh et al. (2020a) demonstrated the presence of the largest glacial lakes and highest GLOF risk in the Eastern Himalaya. For instance, the 100-y flood volume and discharge are both more than three times greater than the next highest region. Despite the unequivocal GLOF risk in the Eastern Himalaya, comprehensive regional studies focusing on magnitude estimation and its impact on downstream life and property are rare. Many studies of the Sikkim Himalaya have focused on the quantification of potentially dangerous glacial lakes (PDGL) (Aggarwal et al., 2017; Islam and Patel, 2022; Sharma et al., 2018; Shukla et al., 2018). Among the few studies focusing on the frequency and magnitude of GLOF (Veh et al., 2020a), Sattar et al. (2019, 2021) modeled the current and future GLOF risk of the largest glacial lake in Sikkim (i.e., South Lhonak Lake). No information, however, is currently available regarding GLOF magnitude from other PDGL in Sikkim Himalaya. Here, we present a pragmatic approach to assessing the state of glacial lakes in terms of GLOF hazard and dam break modeling (DAMBRK). To this end the objectives of present study are 1) to generate an up-to-date inventory of glacial lake in Sikkim Himalaya, 2) a GLOF hazard assessment to identify PDGL, and 3) dam break modelling of PGDL to estimate the potential magnitude of the outburst floods.

2. Materials and methods

2.1. Study site

We focus on the small, state of Sikkim, India, located in Eastern Himalaya (Fig. 1). Covering an area of 7096 km^2, Sikkim shares its borders with Bhutan to the East, Nepal to the West, West Bengal to the South, and Tibet to the North. (Fig. 1). Geographically, Sikkim is situated at the transboundary of Central and Eastern Himalaya. This complex climatological region sits at the triple junction of three climate systems dominated by the Indian Summer Monsoon (ISM), with limited moisture from Westerlies and Easterlies. Long-term climatic observations at Gangtok station exhibit a positive trend in minimum temperature (+0.036 °C) from 1961 to 2017 (Kumar et al., 2020). The small Himalayan state has an altitudinal range from ~280 to 8586 m above sea level (masl), steep slope (> 43% area) and escarpments with rugged terrain. Sikkim hosts the world's third-highest peak, Kangchenjunga (8586 m), 446 glaciers covering 505 km^2 of area as per the Randolph Glacier Inventory (RGI) version 7 (RGI Consortium, 2023), and more than 200 glacial lakes. Snow covers over 35–40% of the Sikkim year-round (Krishna, 2005). The motivation for studying GLOF in this region arises from the presence of Chungthang town, with a population of ~10,000, and the Teesta Stage III hydropower dam, located ~70 km downstream of many PDGL.

2.2. Satellite data

We utilize multisource remote sensing data for mapping glacial lake extent and GLOF hazard assessment. The dataset used for mapping consists of 5 bands (B, G, R, NIR and SWIR) of Sentinel 2, a coherence layer derived using Sentinel 1 (SLC, IWS), Landsat 8 (L1TP, TIRS1), topographic layers (slope and elevation) obtained via Advanced Land Observing Satellite Digital Elevation Model (ALOS DEM); and finally, Normalized Difference Water Index (NDWI) layer. Further details are provided in Table S1.

2.3. Meteorological data

We use time-series meteorological data (total precipitation, mean maximum temperature, and mean minimum temperature) acquired at the Indian Meteorological Department's Automatic Weather Stations (AWSs) situated at Gangtok (1812 m asl) and Mangan (1166 m asl) (Figs. 1 and 2). The Gangtok station has data available from 1990 to 2017 and Mangan station from 2001 to 2017.

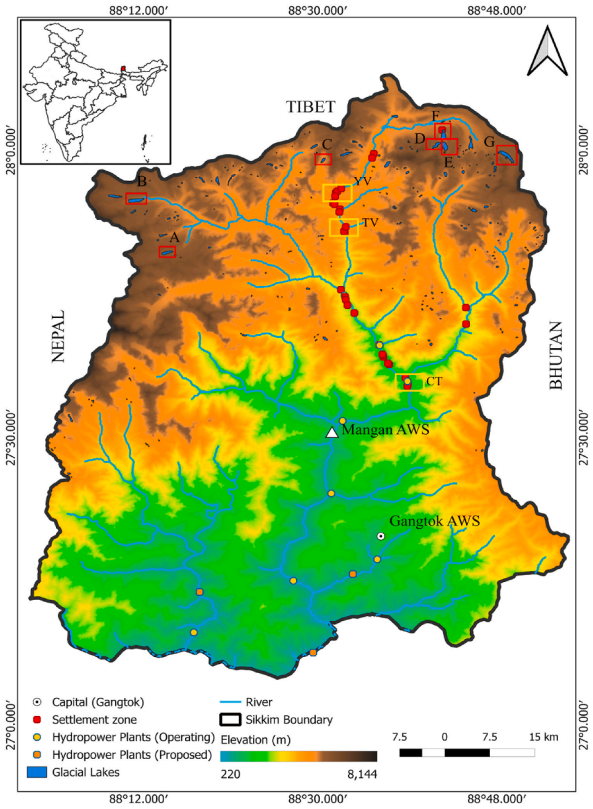

Fig. 1. Location map of Sikkim. The inset map shows the location Sikkim. The Glacial Lakes marked with red polygon (A: Changsang Lake, B: South Lhonak lake, C: Yongdi Lake, D: Ponggu La Lake, E: Za La lake, F: Gurudongmar Lake, and G: Khanchung Lake) provides contextual information for Fig. 7. The yellow polygon (YV: Yongdi Village, TV: Thangu Valley, CT: Chungthang town) provides contextual information for Section 3.2. The map also shows the location of hydropower plants and Automatic Weather Stations (AWS). The Copernicus 30 m Digital Elevation Model (GLO-30) is utilized to show the elevation and deriving stream network. (For interpretation of the references to colour in this figure legend, the reader is referred to the Web version of this article.)

2.4. Other data

OpenStreetMap data (https://www.openstreetmap.org) is utilized to map settlement zones and quantify the infrastructure downstream from glacial lakes. However, OpenStreetMap found to have limited feature coverage in parts of 'Third Pole' (T. Zhang et al., 2023). Thereby, we also manually checked and supplemented the feature for the study region using google earth imagery. The glacial lake boundaries of 1990 are adopted from Zheng et al. (2021) to estimate the rate of lake change from 1900 to 2000. For analysing the terrestrial water storage (TWS) change, the monthly mascon solutions of the Center for Space Research (CSR) Gravity Recovery and Climate Experiment (GRACE) TWS anomalies (TWSA) release 06 version 02 (Save et al., 2016) are used. The datasets are downloaded from https://www2.csr.utexas.edu/grace/RL06_mascons.html. This study utilized the mascon solutions from April 2002 to June 2017 of GRCAE and June 2018 to May 2023 of GRCAE-FO (GFO) available at $0.25^{\circ} \times 0.25^{\circ}$ grid resolution. The provided dataset has applied all appropriate corrections by the agency. For analysing the long-term trend in TWSA, we employed a non-parametric Seasonal-Trend decomposition procedure based on the Loess (STL) approach, as introduced by (Cleveland et al., 1990). This method allowed us to break down the time series data into three components: long-term variability, seasonal variations, and residuals.

2.5. Glacial lake mapping and GLOF hazard assessment

We prepared an inventory of glacial lakes using a Deep Convolutional Neural Network (DCNN; GLNet) as described in Kaushik et al. (Kaushik et al., 2022). GLNet is trained over different sites across the Himalayan region, integrating capabilities of multisource remote sensing data and DCNN. Overall, this lightweight model demonstrated stability for mapping smaller glacial lakes (>0.1 km^2). The results obtained using GLNet are visually inspected for errors of omission or commission. The area error associated with glacial lake mapping using remote sensing data is approximately ± 0.5 subject to the quality of imagery. The error of individual lake is estimated using method proposed by (Hanshaw and Bookhagen, 2014; Xin Wang et al., 2020) using equations (1)–(3).

$$\text{Error } (1\sigma) = \frac{P \times G}{2} \times 0.6872 \tag{1}$$

$$E = \frac{\text{Error } (1\sigma)}{A} \times 100\% \tag{2}$$

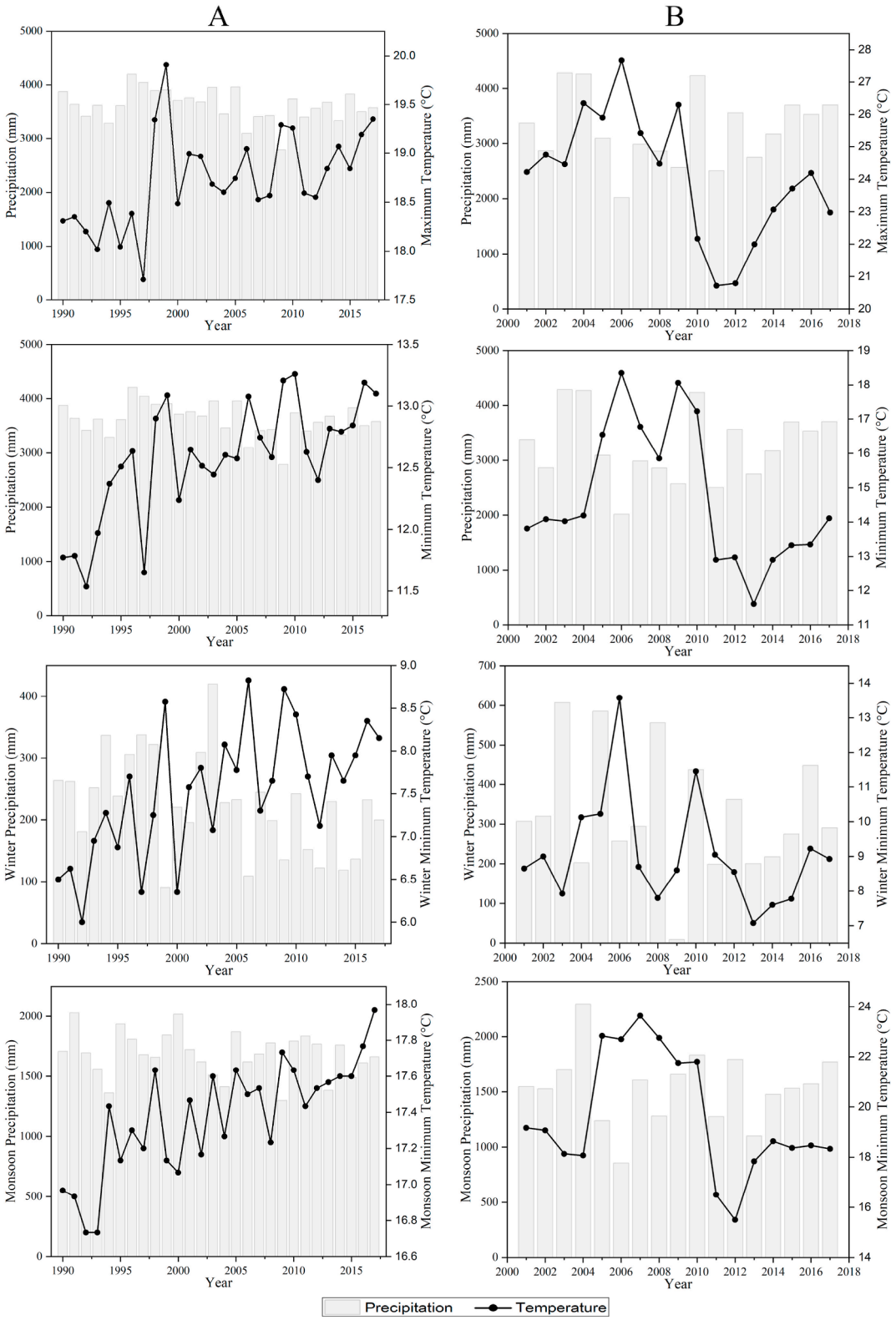

Fig. 2. (A) Long-term variability in climate data observed at Gangtok Automatic Weather Station (AWS) at Annual and seasonal scale from 1990 to 2017 (B) Climatic variability observed at Mangan AWS at Annual and seasonal scale from 2000 to 2012.

$$E_T = \sqrt{\sum_{i=1}^{n} a_i^2} \tag{3}$$

Where, P = perimeter of glacial lake, G = spatial resolution of satellite image used, 0.6872 = revised coefficient used within 1σ, E = relative error of individual glacial lake, A = total area of glacial lake, E_T = error estimated for the entire study area, i = number of lakes, a = area error estimated for single lake.

Here we use the resulting glacial lake inventory for the Sikkim Himalaya to assess and classify glacial lakes in terms of GLOF hazard. Past GLOF hazards in the Himalaya are mostly associated with moraine-dammed glacial lakes (Lalande et al., 2021; Veh et al., 2019). Thus, we focus on such glacial lakes (105 in Sikkim Himalaya) to assess GLOF hazards. A multiple criteria evaluation analysis is employed using AHP (Figs. 3 and 4). The most crucial step in GLOF hazard assessment is selection of assessment parameters. Our selection of assessment parameters is dependent on scientific investigations by previous studies and applicability over large region (T. Zhang et al., 2022; Zheng et al., 2021). There is general consensus within scientific community regarding four most important factors (1: Lake area, 2: Watershed area of upstream lake, 3: downstream slope, 4: slope above lake) for identification of potential dangerous lakes at large scale (Simon Keith Allen et al., 2019; T. Zhang et al., 2022; Zheng et al., 2021). In addition we incorporated two more factors (Shape Index and rate of lake change) based on the previous observations that most of GLOF event in Himalaya are closely associated with rapidly growing moraine dammed glacial lakes which are of usually elongated shapes compared to newly formed circular lakes (Peng et al., 2023; Xue Wang et al., 2024; Zheng et al., 2021).

1) Lake area is calculated to estimate potential maximum GLOF flood magnitude.
2) The mean slope angle of the land above the lake provides the topographic potential of ice and/or rock falling (i.e., ice and/or rock avalanches) into lake, with a slope >30° indicating a high possibility of avalanches to the lake.

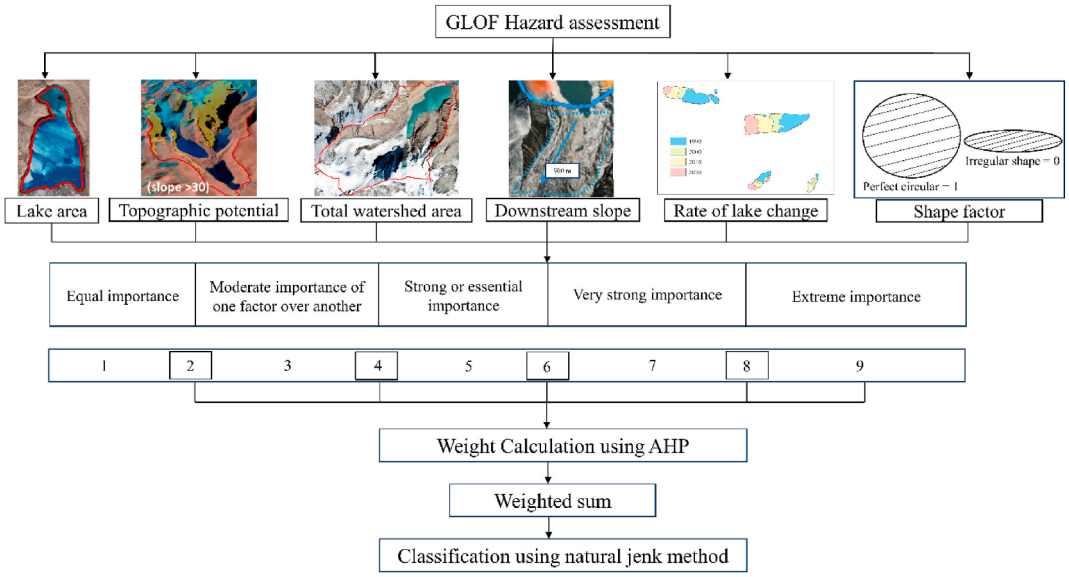

Fig. 3. Pairwise comparison matrix of factors affecting Glacial Lake Outburst Flood (GLOF).

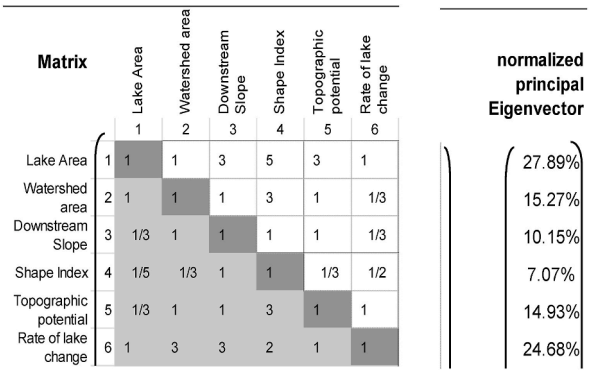

Fig. 4. Weight computation of each factor using Analytical Hierarchical Process (AHP).

3) Total watershed area of the upstream lake is used to incorporate the contribution of precipitation and glacier melt runoff toward the lake and trigger overflow.
4) The downstream slope is generally considered an important factor for lake dam stability and potential outburst flood. This factor is computed as a downstream slope averaged over distance of each lake in three different buffer zones as per lake area (A) ($A \geq 0.1$ km^2, 900m; $0.1 > A \geq 0.05$ km^2, 600m; $0.05 > A \geq 0.01$ km^2, 300m).
5) The rate of lake surface area changes between 1990 and 2020, which provides a measure of long-term stability.
6) The shape index (SI) indicates origin of a lake; More circular glacial lakes with well-defined basin are formed by ancient glacier carving (usually known as cirque lakes). On the other hand, ellipsoidal-shape lakes can be closely associated with supraglacial and proglacial lakes, formed by direct glacier terminus melting and adapting to its form. The range of SI varies between 0 and 1, where 1 represent perfect circular shape of lake and 0 indicate more irregular shape. The more irregular shape can also be associated with the lake stability. The SI is calculated as ($SI = \rho_i / 2\sqrt{\pi a_i}$).

The weights of each of these factors are computed using Analytic Hierarchy Processes AHP (Fig. 3) after normalizing each factor by their range of values. The lakes are then classified by their weighted sum into five levels of GLOF hazard (very high, high, medium, very low, low) using the natural breaks (Jenks) method (Zheng et al., 2021).

2.6. GLOF modelling

In order to understand the detailed impact of GLOF at the study region we have applied GLOF modelling techniques. The combination of models used in this study allows us to evaluate the GLOF hazard potential for every lake found in our study area. Increased recurrence of floods due to the global increase in frequency of extreme precipitation (Snowfall/Rainfall) events present a challenge for hydrological models used to simulate GLOF (Mishra and Rafiq 2017; Rafiq and Mishra 2018). Hence different models for example, Simplified Dam Breach Model (SMPDBK) and Snow Melt Runoff Model (SRM) were used to quantify these impacts the output from one model served as in put to the second.

The Modified Single Flow model uses D8 algorithm to estimate flow direction from each cell to one of its eight neighboring cells toward the direction of steepest descent (O'Callaghan and Mark, 1984). When a gauge station is not available, we utilize the SRM model to quantify the river discharge (no-breach flow) for the study area. The input data for SRM include monthly snow cover area from Moderate Resolution Imaging Spectroradiometer (MODIS) data (MOD10CM), Temperature and the Lapse Rate was derived by using the methodology adopted by (Rafiq et al., 2019; Romshoo et al., 2018) (Table 1). The simulation result (non-breach flow) from SRM is used an input to SMPDBK. SMPDBK is a flood forecasting model for dam failure, developed by the National Weather Service (NWS) (http://www.rivermechanics.net./). This model is capable of providing firsthand information (peak discharge) on downstream flooding due to a dam break using the minimal amount of data (Table 2) compared to more sophisticated dam break models (Kaushik et al., 2020; Rafiq et al., 2019). Detailed information regarding the models used, along with an example of the river profile and cross-section (Fig. S2), is provided in the supplementary material. The SMPDBK method proved to be pragmatic approach where reconnaissance level results are adequate, and sparsely available data and time to prepare the simulation. Global warming has re-

Table 1
Input parameters required by Snow Melt Runoff Model.

Input Parameter	Source
Snow cover Area	MODIS/Terra snow cover daily product (MOD10CM)
Precipitation (RS GP)	Integrated Multi-satellite Retrievals for GPM (IMERG)
Temperature and Lapse rate	Romshoo et al. (2018)
Basin Area and Elevation (RS A/GE)	Google Earth and SRTM DEM
Degree day coefficient	Romshoo et al. (2018)

Table 2
Input parameters required by the Simplified Dam Breach Model (SMPDBK) model and its source.

Input Parameters	Source
Dam Breach Elevation (HDE)	Quantified using visual Interpretation
Final Breach Elevation (BME)	Quantified using visual Interpretation (subtraction of average depth with highest elevation)
Volume of Reservoir (VOL)	Empirical relation given by (G. Zhang et al., 2023)
Surface Area of Reservoir (SA)	Glacial lake surface mapping using GLNet
Final Breach Width (BW)	computed using given equation. $B_w = 0.1803 K_0 (V_w)^{0.32} (h_b)^{0.19}$ (4) (Froehlich, 1995)
Time of Dam Failure (TFM)	computed using given equation. $(T_f)\ \text{in h} = 0.00254\,(V_w)^{0.53}\,(h_b)^{-0.9}$ (5) (Froehlich, 1995)
Non-Breach Flow (QO)	Snow Melt Runoff Model
Distance to PT of Interest (DISTTN)	Estimated distance between Lake outlets and Chungthang town.
Dead Storage Equiv. Mann. N (CMS)	The "0″ value shows Dead Storage when assuming complete drainage from the dam. In the study region, Manning's N ranges from 0.03 to 0.055.
River cross sections	Mapped using google earth
River profile	Mapped using google earth

sulted in a >50% increase in extreme precipitation events in northeastern India since 1990 (Mishra 2019; Mishra et al., 2019). GLOF simulations in the subject areas were carried out for two scenarios: Normal Event (NE) and Extreme Event (NEx). The possible non-breach flow (flow due to heavy precipitation before a GLOF event) from the heavy precipitation events have been incorporated in the extreme event scenario (NEx) using the discharge from SRM. We have also quantified the likely impacts of the snow melt contribution, which can contribute towards the discharge, and incorporated them in the scenario NEx (Rafiq et al., 2019). In this study we have used multiple models including SRM and SMPDBK, for estimation of peak discharge, 1D unsteady flow model developed by Fread was used for the estimation of discharge at the selected locations (which mostly are the populated areas), peak flood depth and the travel time at these downstream locations. The input parameters required by these models (Tables 1 and 2), were obtained from the satellite data, Ancillary data/already published and the data obtained from other models. Overall workflow of adopted methodology is shown in Fig. 5.

2.7. Statistical analyses of climate data

Trend analysis is performed on the AWS data located at Gangtok (1822 m. asl) and Mangan (~1166 m. asl). The non-parametric Man-Kendall and Sen's slope tests were applied to estimate the trend in climate data. The Mann-Kendell test relies on basic assumption that there is no significant trend (H_0) within the time-series data. Thereby, the rejection of null hypothesis (H_0) specifies a significant trend within time-series data. Positive Z_s values reflect an increasing trend within a data series whereas a negative value of Z_s shows a decreasing trend. The statistical analysis is implemented at a 95% confidence interval. The Mann-Kendell test is suitable as it does not require normally distributed dataset and reduces the error introduced by non-uniformity within time-series data (Mishra et al., 2014). Therefore, this statistical test has wide applicability in trend analysis over long-term hydrological and climatological datasets, especially for noisy data with non-linear trends (Kumar et al., 2020; Mishra et al., 2014).

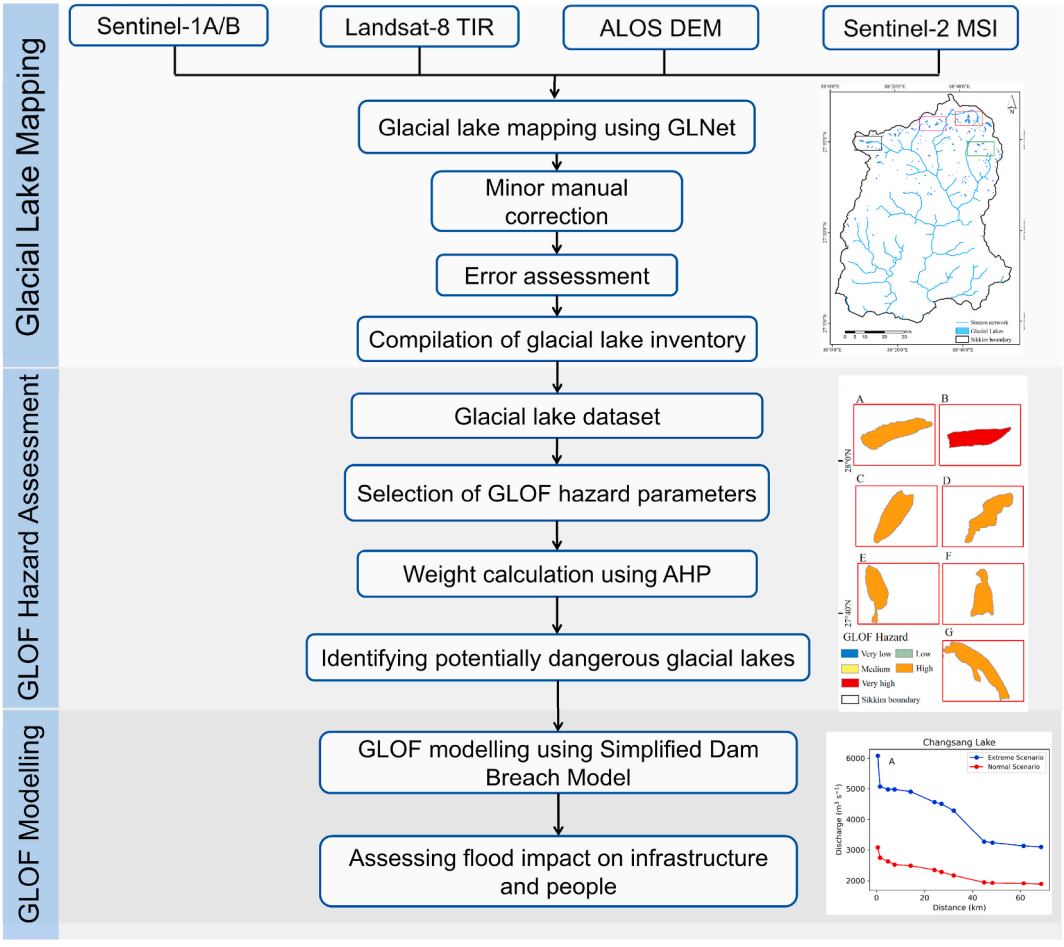

Fig. 5. Overall workflow of the adopted methodology.

3. Results

3.1. Glacial lake inventory and GLOF hazard assessment

Our study identifies 232 glacial lakes in the Sikkim Himalaya covering an area of 22.23 ± 0.10 km^2. Results are restricted to glacial lakes of ≥0.1 km^2 in size and within a buffer zone (10 km) of the glacier margin (Fig. 6). The error assessment reveals absolute area error of approximately ±0.10 km^2 and average relative error ±8.9% in the study region. The relative error of lakes varies within 1.8%–20.7%, our analysis reveals significant power exponential relationship between relative error and lake size (Fig. 7). Our GLOF hazard assessment for the Sikkim Himalaya identifies 18 glacial lakes with a very low level of GLOF hazard, 56 glacial lakes (~50%) with a low hazard, 22 glacial lakes with a medium GLOF hazard, and eight glacial lakes with a high GLOF hazard in the (Fig. 8 and Table 3). Only one glacial lake is identified as having a very high GLOF hazard. To quantify the sensitivity of the weighting scheme in the GLOF hazard assessment, these results are compared to those obtained from an equal weighting scheme (Table 3). The equal weighting scheme method identifies 4 glacial lakes at very high risk and 21 at high risk of GLOF. However, the present work highlights that the AHP method provides an edge to the other method as it allows the expert to rank the factors based on his prior expertise. Such expert knowledge is processed for reducing the subjectivity, if any, and compute objective weights. Moreover, the historical GLOF event shows that a few factors (e.g., size of lake, topographic movement and rapid expansion of glacial lakes) play a more critical role in triggering GLOF events (Zhang et al., 2023). Thereby, giving equal importance to all factors may not reveal the actual picture of GLOF hazard in the region.

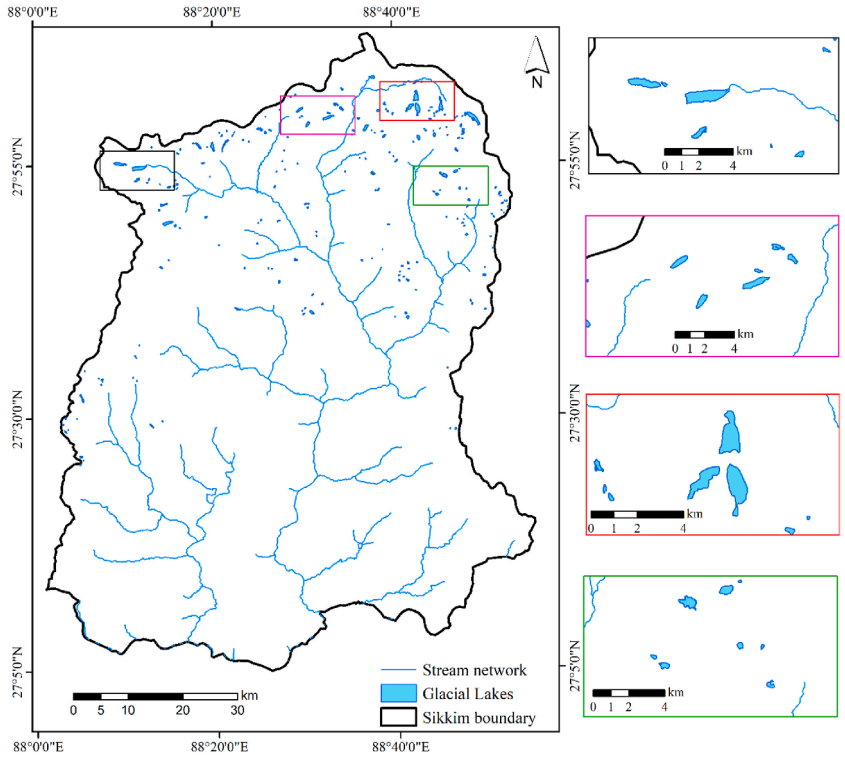

Fig. 6. Glacial Lake dataset generated over the Sikkim Himalaya. The stream network is extracted from the STRM 30 m DEM using the hydrological modeling software in ArcGIS.

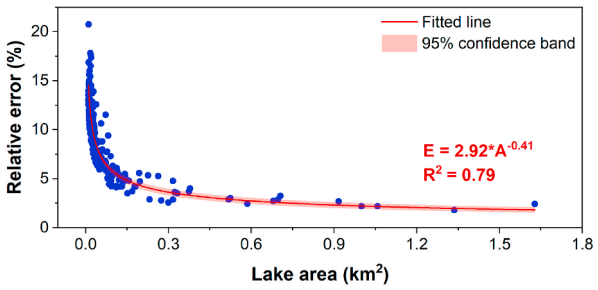

Fig. 7. Relationship between estimated relative error and size of glacial lakes in the study region.

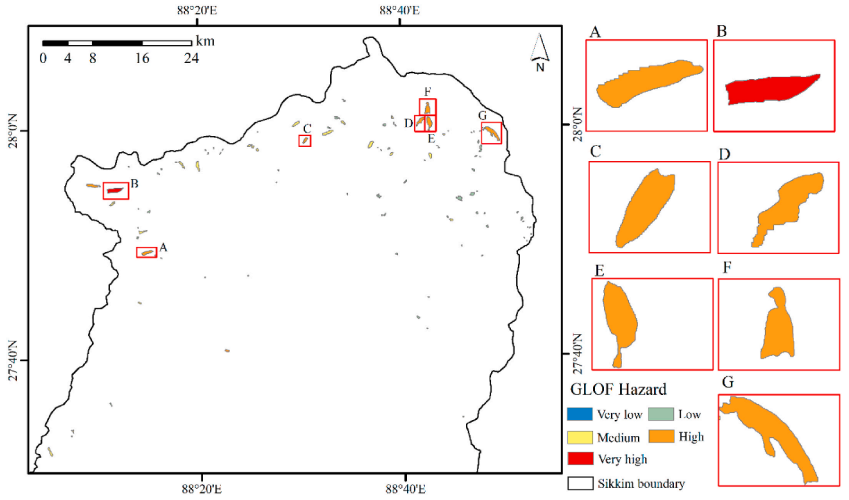

Fig. 8. Glacial Lake Outburst Flood hazard assessment in Sikkim Himalaya. The glacial lakes shown in the insets (A: Changsang Lake, B: South Lhonak lake, C: Yongdi Lake, D: Ponggu La Lake, E: Za La lake, F: Gurudongmar Lake, and G: Khanchung Lake) are modeled using dam break modelling to estimate the potential magnitude of GLOF.

Table 3
A sensitivity analysis for different weighting schemes.

Hazard level	Equal Weighting Scheme	AHP
Very low	16	18
Low	38	56
Medium	26	22
High	21	8
Very high	4	1

3.2. Climatic consideration

The Gangtok weather station has measured an increasing trend of annual mean maximum (0.03 °C yr^{-1}) and mean minimum (0.04 °C yr^{-1}) temperatures, but no significant trend in total annual precipitation (Table 4). For our seasonal analysis, each year is subdivided into four seasons, i.e., winter (December–March), pre-monsoon (April–June), monsoon (July–September) and post-monsoon (October–November). The winter mean maximum and mean minimum temperatures show the fastest rate of increase (0.06 °C yr^{-1}) (Table 4). Mean minimum temperature increased in all seasons; at a rate of 0.04 °C yr^{-1} during pre-monsoon, 0.03 °C yr^{-1} during monsoon, and 0.04 °C yr^{-1} during post-monsoon seasons. A significant trend in precipitation is observed only for the winter season decreasing at a rate of 4.43 mm yr^{-1} (Table 4). In contrast, the Mangan weather station (Table 5) shows no significant trends in annual mean maximum and mean minimum temperatures. However, the mean maximum temperatures decreased by −0.20 °C yr^{-1} during the pre-monsoon season, indicating an increased rate of warming with altitude.

3.3. GLOF modelling

For GLOF simulations, we used modelling approaches to estimate the peak discharge for a catastrophic burst at the seven most vulnerable glacial lakes in the study region. Simulations are carried out for two possible scenarios keeping in view the impacts on the precipitation over the subject area. Moreover, we perform one dimensional routing along the flow channel to the final point of interaction (i.e., Chungthang town). The simulations estimate a peak discharge of 7804 m^3 s^{-1} for a normal out-burst (NE), decreasing to 5418 m^3 s^{-1} by Chungthang town. In the case of an extreme event, the peak discharge reaches 9504 m^3 s^{-1} at the lake, decreasing to

Table 4
Statistical analysis of climate data recorded at Gangtok station.

	Mean max. Temperature (1990–2017)			Mean min. Temperature (1990–2017)			Precipitation (1990–2017)		
	Z_s	Q_s	Trend	Z_s	Q_s	Trend	Z_s	Q_s	Trend
Annual	3.20	0.031	Increasing	3.93	0.043	Increasing	−11.82	−1.44	No trend
Winter	3.09	0.06	Increasing	3.46	0.06	Increasing	−2.35	−4.43	Decreasing
Pre-monsoon	0.75	0.01	No trend	2.53	0.04	Increasing	0.33	1.73	No trend
Monsoon	1.27	0.01	No trend	4.50	0.031	Increasing	−1.26	−5.47	No trend
Post-monsoon	0.81	0.017	No trend	2.45	0.039	Increasing	−0.85	−2.65	No trend

Note: Z_s = Mann–Kendall Z statistic; Q_s = Sen's slope; All statistical test is performed on 95% confidence interval.

Table 5
Statistical analysis of climate data recorded at Mangan station.

	Mean max. Temperature (2001–2017)			Mean min. Temperature (2001–2017)			Precipitation (2001–2017)		
	Z_s	Q_s	Trend	Z_s	Q_s	Trend	Z_s	Q_s	Trend
Annual	−1.77	−0.18	No trend	−0.82	−0.07	No trend	0.123	9.81	No trend
Winter	−1.11	−0.15	No trend	−0.90	−0.04	No trend	−0.70	−4.20	No trend
Pre-monsoon	−2.06	−0.20	Decreasing	−1.36	−0.16	No trend	0.70	16.92	No trend
Monsoon	−1.48	−0.19	No trend	−1.32	−0.10	No trend	4.18	0.20	No trend
Post-monsoon	−1.75	−0.26	No trend	−1.03	−0.124	No trend	−0.04	−0.15	No trend

Note: Z_s = Mann–Kendall Z statistic; Q_s = Sen's slope; All statistical test is performed on 95% confidence interval.

6303 $m^3 s^{-1}$ at the point of interaction (i.e., Chungthang town) (Fig. 9G). Similarly, peak discharges and outflow hydrographs are observed for South Lhonak lake, with peak discharges of 6751 $m^3 s^{-1}$ at the lake and 4535 $m^3 s^{-1}$ downstream. The extreme event scenario results in peak discharges of at 8751 $m^3 s^{-1}$ and 5506 $m^3 s^{-1}$ at the lake and point of interaction, respectively (Fig. 9B).

Simulated peak discharge at Za La Lake is 4972 $m^3 s^{-1}$, gradually decreasing downstream to 3115 $m^3 s^{-1}$ at Chungthang town. Za La lake is situated right above Gurudongmar lake, so an extreme event (Nex) outburst event in Za La lake also triggers a GLOF from Gurudongmar lake in our simulations, resulting in a significantly higher peak discharge of 8421 $m^3 s^{-1}$ at the lake, decreasing to 5773 $m^3 s^{-1}$ at the nearest settlement (i.e., Yongdi village), and to of 4656 $m^3 s^{-1}$ at Chungthang town (Fig. 9E). The simulated peak discharge for Gurudongmar lake is 4449 $m^3 s^{-1}$ (NE) and 6149 $m^3 s^{-1}$ (NEx) decreasing downstream to 2818 $m^3 s^{-1}$ and 6319 $m^3 s^{-1}$, respectively (Fig. 9F). The situation at Gurudongmar lake is noteworthy because it is surrounded by two other lakes (Za La Lake and Ponggu La Lake: Fig. 1) that pose a potential risk of multiple, cascading failures. Incorporation of non-breach flow from Za La Lake and Ponggu La Lake in the case of an extreme event may result in a massive, ~20,000 $m^3 s^{-1}$ peak discharge from these three lakes. These lakes could potentially impact other glacial lakes downstream, setting off a cascade of GLOF along their flow direction.

Changsang lake, located at the terminus of Changsang glacier, has estimated peak discharges of 3084 $m^3 s^{-1}$ (NE) and 6084 $m^3 s^{-1}$ (NEx), decreasing to 1891 $m^3 s^{-1}$ and 3098 $m^3 s^{-1}$ respectively at Chungthang town (Fig. 9A). For Ponggu La Lake, the simulated peak discharge is 4607 $m^3 s^{-1}$ at lake site under the NE scenario, gradually decreasing to 2254 $m^3 s^{-1}$ at Chungthang town. For the extreme (NEx) scenario, the peak discharge increases up to 31.4% (6056 $m^3 s^{-1}$), decreasing to 4213 $m^3 s^{-1}$ at Yongdi village and Thangu valley, and 2909 $m^3 s^{-1}$ at Chungthang town (Fig. 9D). Of all seven lakes, the lowest simulated peak discharge was for Yongdi Lake (622 $m^3 s^{-1}$) in case of normal outburst event, decreasing to 447 $m^3 s^{-1}$ at Chungthang town. For the extreme scenario, these model estimates peak discharges of 1572 $m^3 s^{-1}$ at the lake, 1279 $m^3 s^{-1}$ at Yongdi village, and 899 $m^3 s^{-1}$ at Chungthang town (Fig. 9C).

4. Discussion

4.1. Increasing risk of GLOF in a warming climate

The generated dataset of glacial lake boundaries in the present study proved to be more accurate and updated over existing glacial lake datasets generated by (Chen et al., 2021; Zheng et al., 2021). The results of the present study are comparable to Chen et al. (2021) which reports the presence of 234 glacial lakes covering 23.36 km^2 (Table 6). A visual comparison of the glacial lake boundaries mapped in the present study with existing glacial lake datasets (Chen et al., 2021; Zheng et al., 2021) is provided in Fig. 10. The slight variation in the number and areal extent is mainly ascribed to the coarse resolution of the Landsat OLI sensor used for mapping glacial lakes. Whereas our result is restricted to lakes within a 10 km buffer zone of the glacier margin and those with a surface area or ≥0.1 km^2, Zheng et al. (2021) mapped all high altitudinal glacial lakes, resulting in a higher number and extent (Table 6). These recent studies highlighted the higher rate of lake areal enlargement and the doubled risk of GLOF compared to adjacent regions (Veh et al., 2020a; Zheng et al., 2021). Glacial lake expansion in the region is primarily attributed to atmospheric warming and glacier ice mass loss (G. Zhang et al., 2023), which is consistent with the increasing trend in maximum temperature (−0.031 °C yr^{-1}, Table 3) and decreasing trend in winter precipitation (−4.43 mm yr^{-1}) we observe. A similar observation is reported by Kumar et al. (2020), the climatic data recorded at Gangtok station during 1961–2017 reveals increasing trend in minimum (−0.036 °C yr^{-1}) and maximum temperature (−0.027 °C yr^{-1}). Additionally, the long-term analysis of GRACE and GFO data revealed statistically significant decreasing trend at the rate of 0.21 cm $month^{-1}$ water equivalent of mass loss in the region. Fig. 11 shows that rate of mass loss is higher in the glaciated regions indicating higher rate of atmospheric warming in the upper reaches (Mountain Research Initiative EDW Working Group, 2015).

The assessment of GLOF hazards is complex, involving many different parameters of the lake size and shape, its dam characteristics, the parent glacier, topographic potential, tectonic movement, heavy precipitation, and population hotspot in the downstream region. Several researchers have recently demonstrated models and several classification methods to identify PDGL (Aggarwal et al., 2017; Islam and Patel, 2022; Khanal et al., 2015). These studies emphasize the scientific evaluation of GLOF parameters (T. Zhang et al., 2022) and their applicability over large geographical regions using automated approaches (Simon Keith Allen et al., 2019; Zheng et al., 2021). The approach adopted in the present work is based on the findings of previous studies and has applicability over large geographical regions. However, we have added two more parameters (i.e., rate of lake changes and shape index) for GLOF hazard assessment which provides critical information about lake stability. Higher rates of lake change, and shape index values close to zero, indicating ellipsoidal shape, are associated with proglacial lakes.

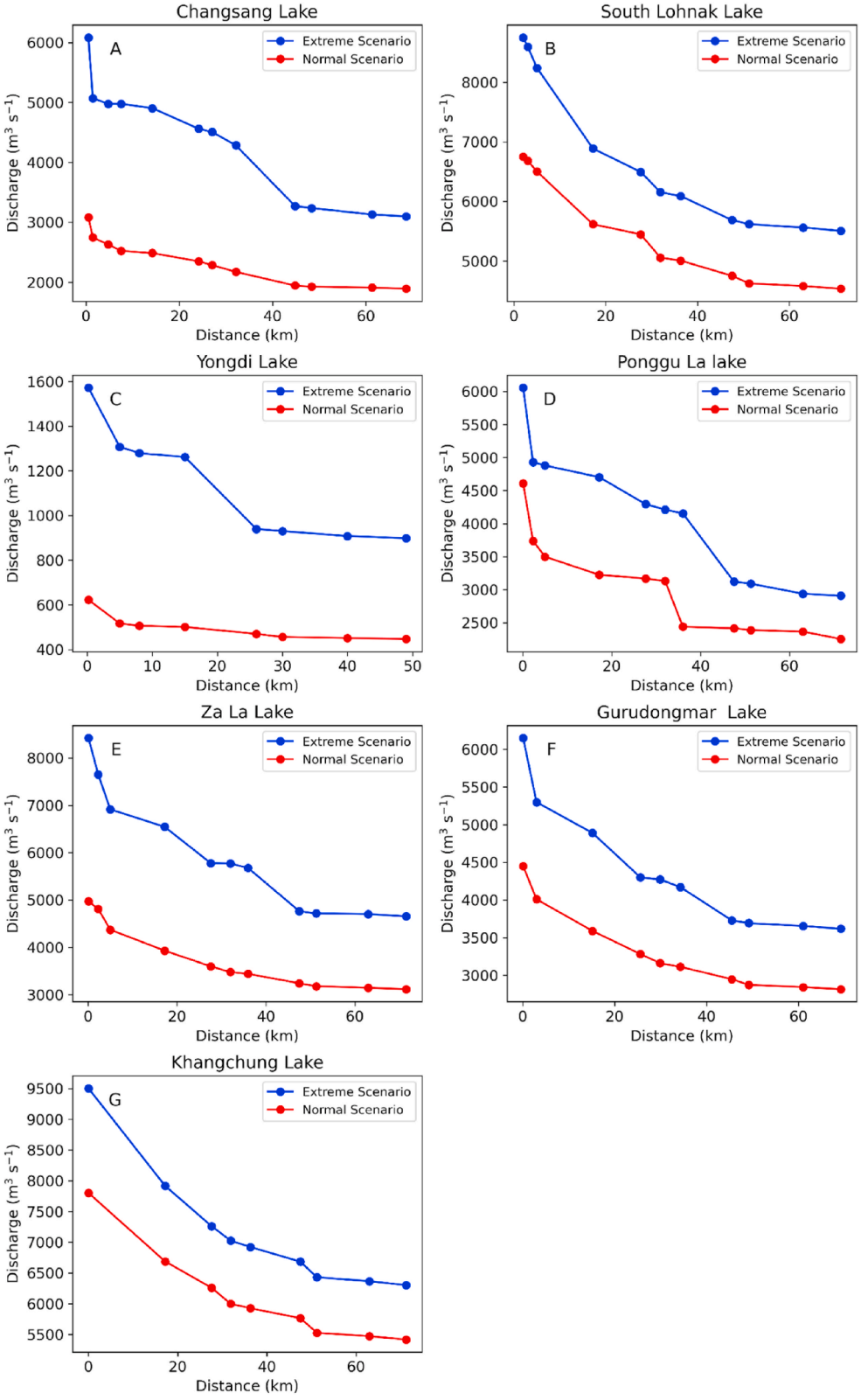
Changsang Lake
A
Extreme Scenario
Normal Scenario
Discharge (m³ s⁻¹)
Distance (km)
South Lohnak Lake
B
Yongdi Lake
C
Ponggu La lake
D
Za La Lake
E
Gurudongmar Lake
F
Khangchung Lake
G

Fig. 9. Outflow hydrographs for the seven most vulnerable glacial lakes in Sikkim exhibiting peak discharges for two different scenarios (NE and NEx). The contextual information of simulated lakes (A: Changsang Lake, B: South Lhonak lake, C: Yongdi Lake, D: Ponggu La Lake, E: Za La lake, F: Gurudongmar Lake, and G: Khanchung Lake) are provided in Fig. 1.

Table 6
Comparison of glacial lake (area and number) reported in the present study with recently published datasets.

Lake dataset	Data used	Numbers of lakes	Total lake area (km^2)
Zheng et al. (2021)	Landsat ETM+ ~2015	338	29.63
Chen et al. (2021)	Landsat OLI ~2017	234	23.36
Present study	Sentinel-2 2020	231	22.23 ± 0.10

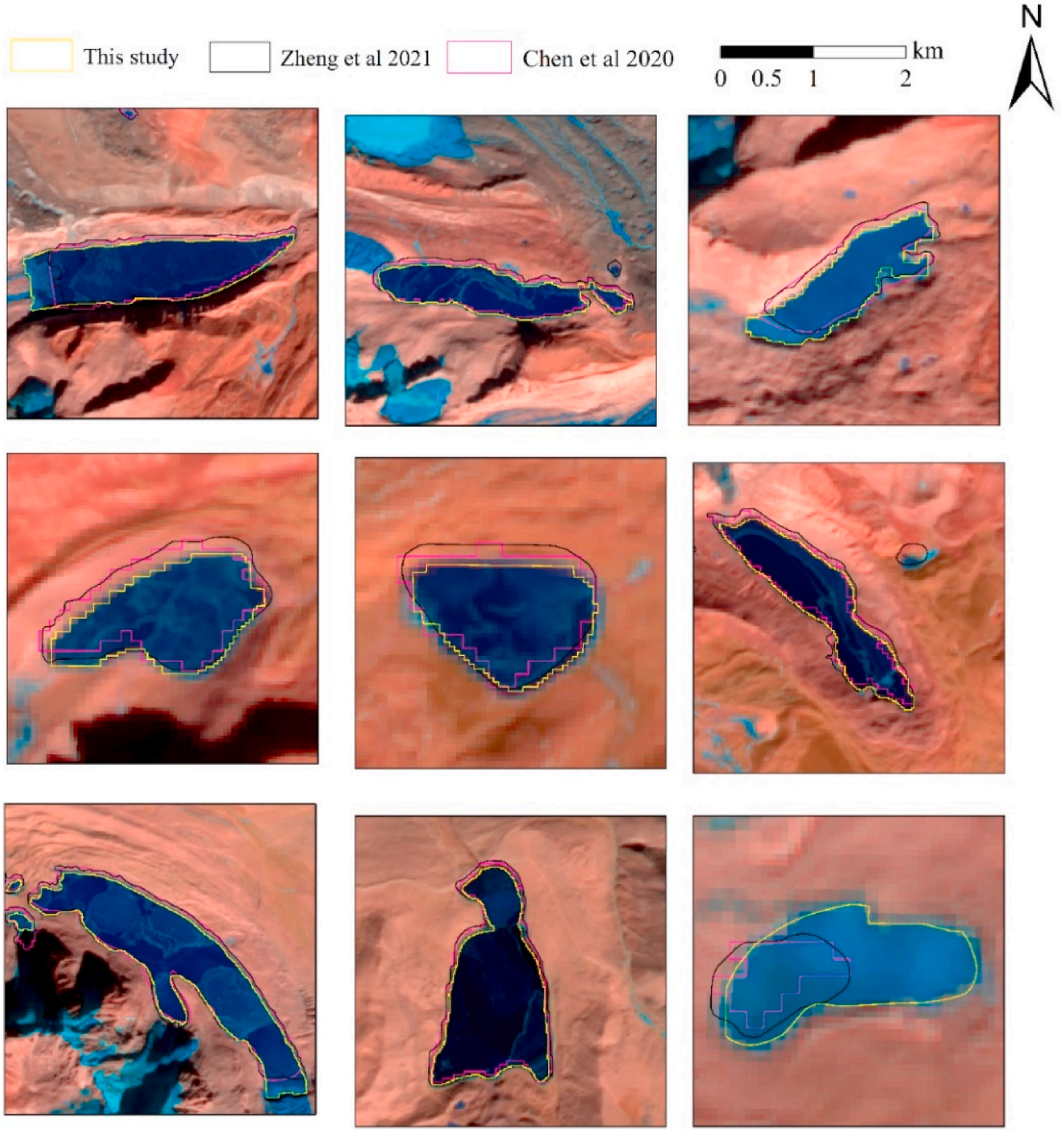

Fig. 10. Comparison of generated glacier lake dataset of Sikkim Himalaya with existing datasets (e.g., Chen et al., 2021; Zheng et al., 2021). The present study provides a generally more accurate mapping of lake extent.

Our results exhibit the presence of 31 potentially dangerous glacial lakes (22; moderate, 8; high, and 1; very high). These findings are consistent with previous studies of the Sikkim Himalaya (Aggarwal et al., 2017; Islam and Patel, 2022). Aggarwal et al. (2017) identified 21 lakes susceptible to outburst flood in Sikkim. Similarly, Islam et al. (2022) investigated the presence of 27 potentially dangerous glacial lakes (17; moderate, 5; high, 5; low) in the Chhombo Chhu Watershed, Sikkim Himalaya. Minor discrepancies in the results can be attributed to the scale of lake mapping, factors included for GLOF hazard assessment, classification categories and

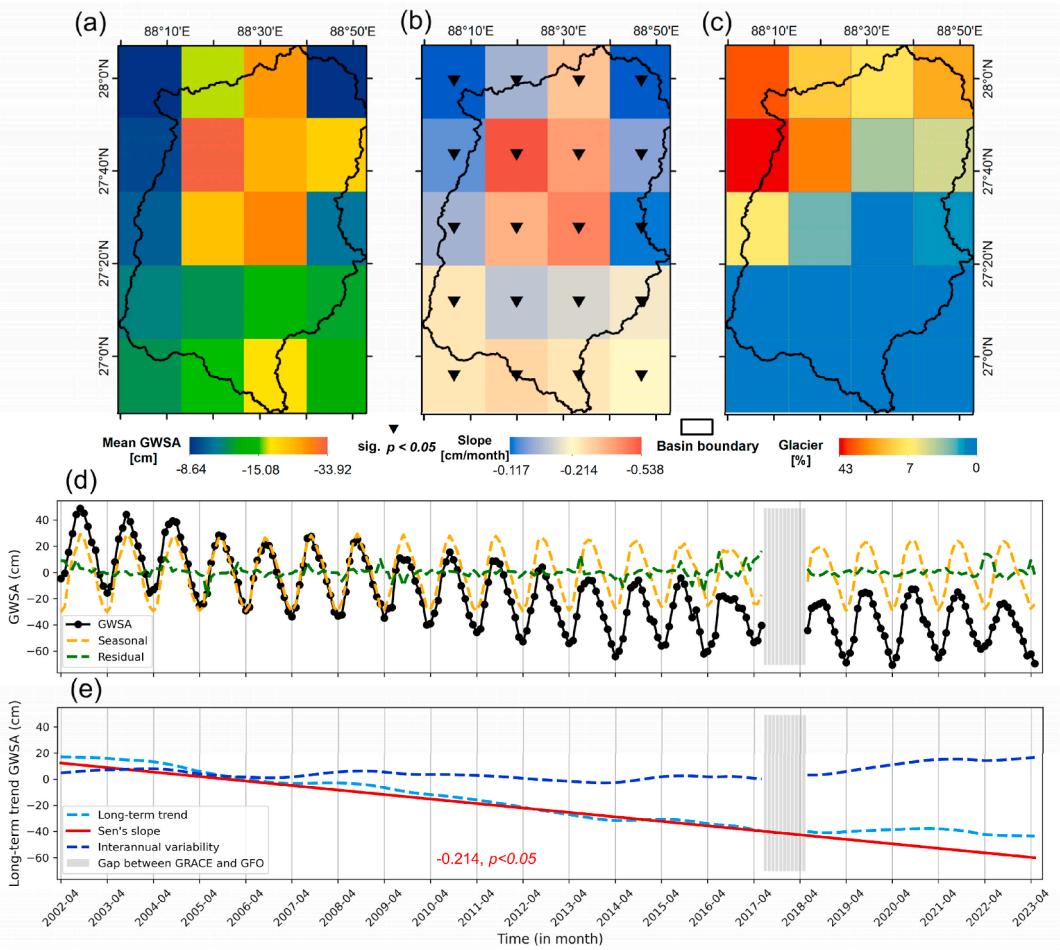

Fig. 11. Spatial distribution of (a) GRACE and GRACE-FO, (b) slope derived through long-term trend analysis, (c) area covered by glacier, (d) temporal distribution of GRACE TWSA, seasonal and residual components, and (e) long-term trend (linear trend and inter-annual variability) during April 2002–May2023.

study region. While Aggarwal et al. (2017) focused on glacial and high altitude lakes, this study focuses on moraine-dammed glacial lakes only. Moreover, Aggarwal et al. (2017) used 16 parameters for GLOF hazard assessment, whereas we adopted a widely accepted conceptual model (Simon Keith Allen et al., 2019; Zheng et al., 2021) for GLOF assessment, with the addition of the rate of lake change and shape index. Zheng et al. (2021) made the notable contribution of estimating the GLOF risk of the entire 'third pole' region. That analysis found that, among the seven glacial lakes modeled here, four are classified as very high GLOF risk (Ponggu La Lake, Za La lake, Khangchung Lake and Yongdi Lake; Gurudongmar lake in missing from the analysis), one identified as a highly dangerous lake (Zheng et al., 2021). However, Zheng et al. (2021) classified South Lhonak lake as low risk lake, which our analysis classifies as high risk. The South Lhonak lake has a lake volume of 65.8 × 106 m^3 and a maximum depth of 131 m (Sharma et al., 2018) and has been identified as one of the most dangerous glacial lake in the Sikkim Himalaya (Aggarwal et al., 2017; Islam and Patel, 2022; Sattar et al., 2019, 2021).

4.2. GLOF drivers and anticipated risk

A GLOF can be triggered by numerous factors, involving dam stability, overtopping, an extreme climate event such as heavy rainfall, seismic activity, avalanches and/or combination of these factors (Sattar et al., 2021; D. H. Shugar et al., 2021; Worni et al., 2013). In the recent past, the Indian Himalaya has witnessed the Kedarnath GLOF event induced by heavy rainfall (S. K. Allen et al., 2016; Rafiq et al., 2019) and the Chamoli disaster caused by avalanche (D. H. Shugar et al., 2021). The potential risk of GLOF event in Sikkim Himalaya due to heavy rainfall, tectonic activity induced avalanches and/or a combination of these factors are equally high. Sikkim is a highly active seismic zone (IV) that has experienced 10 strong earthquakes of magnitude varying between 6.1 and 8.0 during 1990–2023 (https://earthquakelist.org/india/sikkim/). Most concerning were the 4.9 magnitude earthquake on Sept 19, 1991, and 6.9 magnitude on Sept 18, 2011, with epicenters located in the vicinity of the South Lhonak lake (Sattar et al., 2021). Additionally, the topographic potential near the lake (slope >30°), increasing rate of lake formation, and expansion contribute significantly to the anticipated GLOF event in the study region. Recent studies highlight that there is at least twice the risk of GLOF in the Eastern Himalaya compared to its adjacent regions (Veh et al., 2020b; Zheng et al., 2021). In view of these observations, several researchers

have modeled present and future GLOF scenarios (Rinzin et al., 2023; Sattar et al., 2019, 2021). However, most of the studies carried out in the Sikkim Himalaya are either limited to the identification of PGDL or modelling only one lake (i.e., South Lhonak). The present work adopts a comprehensive approach by extending the analysis from identification of PDGL to modelling the magnitude of outburst flood from seven PDG (Fig. 9).

We estimate a GLOF peak discharges for South Lhonak lake (6751 $m^3 s^{-1}$ at the lake, 4535 $m^3 s^{-1}$ at Chungthang town), very similar to those estimated by Sattar et al. (2019) (6064 $m^3 s^{-1}$ and 3828 $m^3 s^{-1}$, respectively). Unlike Sattar et al. (2019), our approach to simulating GLOFs does not include physical and natural barriers that can significantly reduce the flow energy and lower downstream peak discharges. We present the first simulations of GLOF peak discharges for the other six glacial lakes (A: Changsang Lake, C: Yongdi Lake, D: Ponggu La Lake, E: Za La lake, F: Gurudongmar Lake, and G: Khanchung Lake; Fig. 9). The results highlight the significant and increasing risk for high magnitude floods from this understudied part of the Sikkim Himalaya. An outburst flood from Khanhchung lake would likely be high destructive to settlements downstream (Fig. 12 and Fig. S3). GLOF simulations show that population and infrastructure (~120 settlements) are under direct threat, and this risk can exacerbate in the case of extreme events (Fig. 13 and Fig. S3). The estimated peak outflow discharge is significantly higher than what we have witnessed in the past. For example, the Uttarakhand, India flash flood estimated peak discharge was 1699 $m^3 s^{-1}$ which resulted in over 6000 deaths (Rafiq et al., 2019). Similarly, Dig Tsho lake located in Bhutan Himalaya experienced a peak discharge of 1562 $m^3 s^{-1}$ which impacted 30 km downstream of the lake (Gurung et al., 2017).

Our study also highlights the burgeoning GLOF hotspot of the area of Ponggu La, Za La and Gurudongmar Lakes (Fig. 8). Their close proximity to each other increases the threat of a cascading, destructive GLOF event. For example, we have incorporated the outflow of Gurudongmar Lake while simulating the extreme event scenario for Za La Lake which resulted in peak discharge of 8421 $m^3 s^{-1}$. The incorporation of outflow from Gurudongmar lake almost doubles the magnitude of the flood in comparison to the normal case scenario. The GLOF event triggered by hydrometeorological factors (e.g., heavy rainfall) and mass movement (e.g., snow and debris avalanches) may result in a devastating flood involving exceedingly large volumes of water from all three lakes, which have major carrying capacities. Resultant floods could impact hundreds of kilometers down flow, causing loss of life and property at large scales. The outflow hydrographs from other glacial lakes also exhibits a similar potential GLOF event (Fig. 9). Even the outburst event from the smallest lake (C: Yongdi Lake; Figs. 1 and 9) might cause a flash flood with a peak discharge of 506 $m^3 s^{-1}$ reaching to Yongdi village located approximately 8 km downstream of the lake with approximately 110 settlements (Fig. 12). The high possibility of a debris flow alongside the GLOF event may exacerbate the hazard by adding to the flood height because the slope at various locations downstream is well above the threshold where dry, unconsolidated debris can mobilize. Hence these GLOFs can generate catastrophic flash floods that inundate most of the Sikkim, devastating the population and infrastructure downstream. Overall, our results indicate potential GLOF events that directly threaten populations of ~10,000 and critical infrastructure totaling 1900 settlements, 5

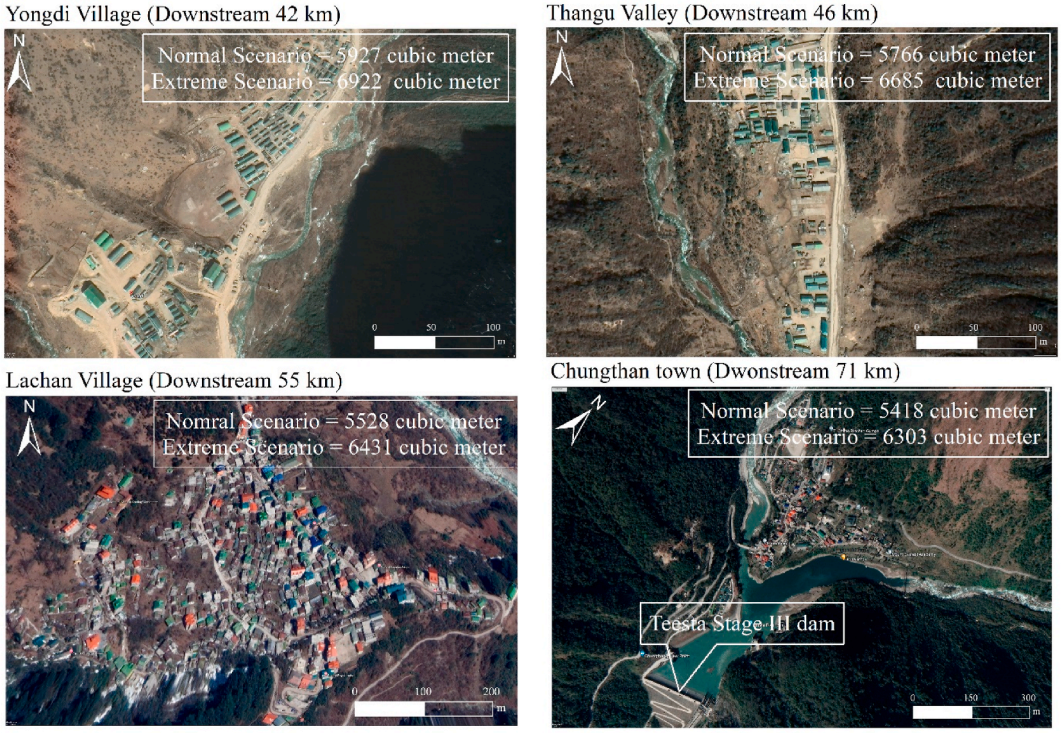

Fig. 12. Major settlement zones under direct threat of potential glacial lake outburst flood. The Magnitude of flood is depicted for Khangchung Lake. The location of settlement zones is shown in Fig. 1. Image source; Google Earth (Image © 2023 Maxar Technologies).

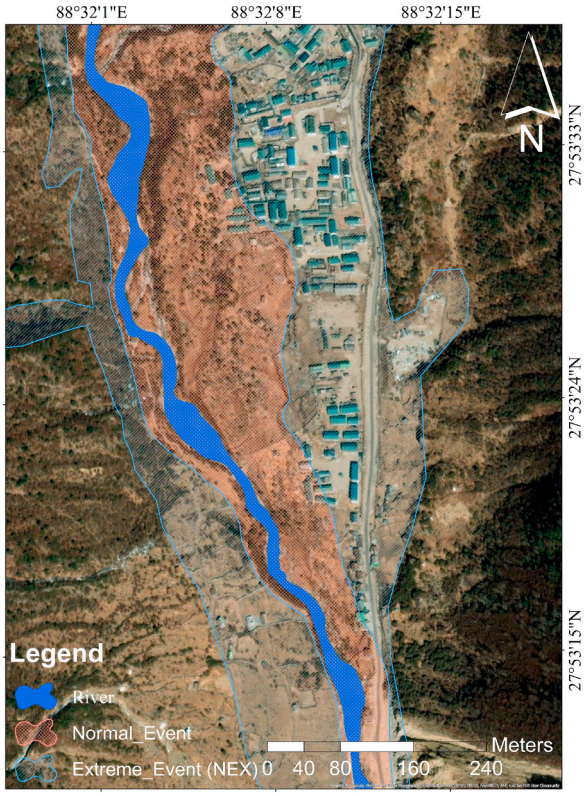

Fig. 13. Modeled flood extent in Thangu Valley (TV) under normal and extreme scenarios from Khanchung Lake. The location TV is shown in Fig. 1. Image source: Google Earth (Image © 2023 Maxar Technologies).

bridges and 2 hydropower plants. The current is that such increasing GLOF risk in high mountain regions is further aggravated by unprecedented infrastructural development activities into the highly vulnerable regions (Kaushik et al., 2020).

4.3. Mitigation strategies

The threat of GLOFs in this region necessitates immediate mitigation strategies that require the combined efforts of the local community, the scientific community, and local administration. Here we restrict our discussion to the measures that can be taken as a part of scientific community. In the pre-GLOF phase, a near real-time glacial lake mapping and monitoring system is required which can facilitate regular glacial lake monitoring at unprecedented scale. There is excellent potential in deep learning models for automated glacial lake mapping (Kaushik et al., 2022; Wang et al., 2022; S. Wang et al., 2022). Also needed is the rapid and accurate identification of potentially dangerous lakes. Both the current study and the automated approaches introduced by (Simon Keith Allen et al., 2019) could be employed for this purpose. Finally, the installation of an early warning system at the most dangerous lake site is needed (W. Wang et al., 2022). Such systems are expensive and difficult to maintain and are impractical for high numbers of PDGL. However, we recommend the installation of early warning systems at the GLOF hotspots with enormous volumes of water and/or proximity to human settlement. Further, in cases of extreme GLOF threat, activities to reduce PDGL volume using control engineering methods are needed. For example, 1) controlled breaching of the dam, 2) construction of a dam outlet, 3) pumping and 4) tunnel construction through dam. Strategic combinations of these efforts will help mitigate the devastating impact of GLOFs and promote sustainable development in the region.

5. Conclusion

The loss of glacier ice and associated formation and expansion of glacial lakes is unequivocal. The increasing number and extent of glacial lakes threaten downstream communities and infrastructure. The impending threat of GLOFs in Sikkim, located in the Eastern Himalaya, is a serious concern that necessitates a pragmatic and comprehensive solution. The objective of this study was to evaluate the state of glacial lakes in the region in terms of GLOF hazard and employ dam break modeling, particularly the DAMBRK model, to project potential GLOF scenarios. By coupling this analysis with the recent inventory of glacial lakes in the Sikkim Himalaya, we aimed to assess GLOF hazards and identify PDGLs, as well as to conduct dam break modeling on high-risk GLOF-prone lakes to estimate the magnitude of a potential outburst flood. This multi-faceted approach is essential for the management and mitigation of GLOF hazards in the region. Our results highlight the increasing risk of GLOF in the Sikkim Himalaya where every simulated scenario for each lake demonstrates an outflow of high volumes of water reaching Chungthang town. The smallest simulated lake shows a dis-

charge of 447 m^3 s^{-1}, whereas the extreme case scenario from Khangchung lake suggests a 6303 m^3 s^{-1} discharge reaching to Chungthang town. The results showed direct exposure of >10,000 people and infrastructure (~1900 settlements and 5 bridges). The data generated from this study will not only provide vital insights into the state of glacial lakes and the risks they pose but also empower local authorities and communities to take pragmatic approach to reduce the potential impact of GLOFs. Additionally, this research can contribute to the development of early warning systems, disaster preparedness plans, and infrastructure improvements aimed at minimizing the damage and reducing the risk to human life in the occurrence loss a GLOF. As climate change continues to accelerate, and glaciers in the Himalayan region continue to recede, the threat of GLOFs is expected to increase. Therefore, ongoing monitoring and proactive risk assessment will be essential to safeguard the lives and livelihoods of the thousands of people living in the region. By combining advanced modeling techniques with up-to-date inventory data, this study offers a practical and invaluable foundation for addressing this pressing issue and striving for a safer, more resilient future for Sikkim and its inhabitants.

Ethical Statement for Solid State Ionics

Hereby, I Saurabh Kaushik consciously assure that for the manuscript Increasing risk of glacial lake outburst flood in Sikkim, Eastern Himalaya under climate warming the following is fulfilled:

1)This material is the authors' own original work, which has not been previously published elsewhere.
2)The paper is not currently being considered for publication elsewhere.
3)The paper reflects the authors' own research and analysis in a truthful and complete manner.
4)The paper properly credits the meaningful contributions of co-authors and co-researchers.
5)The results are appropriately placed in the context of prior and existing research.
6)All sources used are properly disclosed (correct citation). Literally copying of text must be indicated as such by using quotation marks and giving proper reference.
7)All authors have been personally and actively involved in substantial work leading to the paper, and will take public responsibility for its content.
The violation of the Ethical Statement rules may result in severe consequences.

To verify originality, your article may be checked by the originality detection software iThenticate. See also http://www.elsevier.com/editors/plagdetect.

I agree with the above statements and declare that this submission follows the policies of Solid State Ionics as outlined in the Guide for Authors and in the Ethical Statement.

CRediT authorship contribution statement

Saurabh Kaushik: Writing – review & editing, Writing – original draft, Methodology, Formal analysis, Data curation, Conceptualization. **Mohammd Rafiq:** Writing – review & editing, Methodology, Formal analysis. **Jaydeo K. Dharpure:** Writing – review & editing, Methodology, Formal analysis. **Ian Howat:** Writing – review & editing, Conceptualization. **Joachim Moortgat:** Writing – review & editing, Conceptualization. **P.K. Joshi:** Writing – review & editing, Conceptualization. **Tejpal Singh:** Writing – review & editing, Conceptualization. **Andreas J. Dietz:** Writing – review & editing, Conceptualization.

Declaration of competing interest

The authors declare that they have no known competing financial interests or personal relationships that could have appeared to influence the work reported in this paper.

Data availability

Data will be made available on request.

Acknowledgment and Data Availability Statement

The Sentinel data used for glacial lake mapping is available from https://apps.sentinel-hub.com/. The glacial lake mapping data used for comparison is available at https://doi.org/10.6084/m9.figshare.21708590 and https://doi.org/10.5281/zenodo.4275164. Data used for mapping settlement zone and downstream infrastructure is accessible from https://www.openstreetmap.org. GRACE TWS dataset is downloaded from https://www2.csr.utexas.edu/grace/RL06_mascons.html. Climate data is procured from Indian Meteorological Department-Met Centre Gangtok; this dataset may be provided for scientific purpose upon author request. GLOF simulation tools are available at http://www.rivermechanics.net./

Appendix A. Supplementary data

Supplementary data to this article can be found online at https://doi.org/10.1016/j.rsase.2024.101286.

References

Aggarwal, S., Rai, S.C., Thakur, P.K., Emmer, A., 2017. Inventory and recently increasing GLOF susceptibility of glacial lakes in Sikkim, Eastern Himalaya. Geomorphology 295, 39–54. https://doi.org/10.1016/j.geomorph.2017.06.014.

Allen, S.K., Rastner, P., Arora, M., Huggel, C., Stoffel, M., 2016. Lake outburst and debris flow disaster at Kedarnath, June 2013: hydrometeorological triggering and topographic predisposition. Landslides 13 (6), 1479–1491. https://doi.org/10.1007/s10346-015-0584-3.

Allen, Simon Keith, Zhang, G., Wang, W., Yao, T., Bolch, T., 2019. Potentially dangerous glacial lakes across the Tibetan Plateau revealed using a large-scale automated assessment approach. Sci. Bull. 64 (7), 435–445. https://doi.org/10.1016/j.scib.2019.03.011.

Brun, F., Berthier, E., Wagnon, P., Kääb, A., Treichler, D., 2017. A spatially resolved estimate of High Mountain Asia glacier mass balances from 2000 to 2016. Nat. Geosci. 10 (9), 668–673. https://doi.org/10.1038/ngeo2999.

Chen, F., Zhang, M., Guo, H., Allen, S., Kargel, J.S., Haritashya, U.K., Watson, C.S., 2021. Annual 30 m dataset for glacial lakes in high mountain Asia from 2008 to 2017. Earth Syst. Sci. Data 13 (2), 741–766. https://doi.org/10.5194/essd-13-741-2021.

Cleveland, R.B., Cleveland, W.S., McRea, J.E., Terpenning, I., 1990. STL: a seasonal-trend decomposition procedure based on loess. J. Off. Stat. 6 (1), 3–73.

Dehecq, A., Gourmelen, N., Gardner, A.S., Brun, F., Goldberg, D., Nienow, P.W., et al., 2019. Twenty-first century glacier slowdown driven by mass loss in High Mountain Asia. Nat. Geosci. 12 (1), 22–27. https://doi.org/10.1038/s41561-018-0271-9.

Froehlich, D.C., 1995. Peak outflow from breached embankment dam. J. Water Resour. Plann. Manag. 121 (1), 90–97.

Gurung, D.R., Khanal, N.R., Bajracharya, S.R., Tsering, K., Joshi, S., Tshering, P., et al., 2017. Lemthang Tsho glacial Lake outburst flood (GLOF) in Bhutan: cause and impact. Geoenviron. Disasters 4 (1), 17. https://doi.org/10.1186/s40677-017-0080-2.

Hanshaw, M.N., Bookhagen, B., 2014. Glacial areas, lake areas, and snow lines from 1975 to 2012: status of the Cordillera Vilcanota, including the Quelccaya Ice Cap, northern central Andes, Peru. Cryosphere 8 (2), 359–376. https://doi.org/10.5194/tc-8-359-2014.

Huggel, C., Haeberli, W., Kääb, A., Bieri, D., Richardson, S., 2004. An assessment procedure for glacial hazards in the Swiss Alps. Can. Geotech. J. 41 (6), 1068–1083. https://doi.org/10.1139/t04-053.

Hugonnet, R., McNabb, R., Berthier, E., Menounos, B., Nuth, C., Girod, L., et al., 2021. Accelerated global glacier mass loss in the early twenty-first century. Nature 592 (7856), 726–731. https://doi.org/10.1038/s41586-021-03436-z.

Islam, N., Patel, P.P., 2022. Inventory and GLOF hazard assessment of glacial lakes in the Sikkim Himalayas, India. Geocarto Int. 37 (13), 3840–3876. https://doi.org/10.1080/10106049.2020.1869332.

Kaushik, S., Rafiq, M., Joshi, P.K., Singh, T., 2020. Examining the glacial lake dynamics in a warming climate and GLOF modelling in parts of Chandra basin, Himachal Pradesh, India. Sci. Total Environ. 714, 136455. https://doi.org/10.1016/j.scitotenv.2019.136455.

Kaushik, S., Singh, T., Joshi, P.K., Dietz, A.J., 2022a. Automated mapping of glacial lakes using multisource remote sensing data and deep convolutional neural network. Int. J. Appl. Earth Obs. Geoinf. 115, 103085. https://doi.org/10.1016/j.jag.2022.103085.

Kaushik, S., Singh, T., Bhardwaj, A., Joshi, P.K., 2022b. Long-term spatiotemporal variability in the surface velocity of Eastern Himalayan glaciers, India. Earth Surf. Process. Landforms 5342. https://doi.org/10.1002/esp.5342.

Khanal, N.R., Mool, P.K., Shrestha, A.B., Rasul, G., Ghimire, P.K., Shrestha, R.B., Joshi, S.P., 2015. A comprehensive approach and methods for glacial lake outburst flood risk assessment, with examples from Nepal and the transboundary area. Int. J. Water Resour. Dev. 31 (2), 219–237. https://doi.org/10.1080/07900627.2014.994116.

Krishna, A.P., 2005. Snow and glacier cover assessment in the high mountains of Sikkim Himalaya. Hydrol. Process. 19 (12), 2375–2383. https://doi.org/10.1002/hyp.5890.

Kumar, P., Sharma, M.C., Saini, R., Singh, G.K., 2020. Climatic variability at Gangtok and Tadong weather observatories in Sikkim, India, during 1961–2017. Sci. Rep. 10 (1), 15177. https://doi.org/10.1038/s41598-020-71163-y.

Lalande, M., Ménégoz, M., Krinner, G., Naegeli, K., Wunderle, S., 2021. Climate change in the high mountain Asia in CMIP6. Earth Syst. Dynamics 12 (4), 1061–1098. https://doi.org/10.5194/esd-12-1061-2021.

Lee, E., Carrivick, J.L., Quincey, D.J., Cook, S.J., James, W.H.M., Brown, L.E., 2021. Accelerated mass loss of Himalayan glaciers since the little ice age. Sci. Rep. 11 (1), 24284. https://doi.org/10.1038/s41598-021-03805-8.

Maurer, J.M., Schaefer, J.M., Rupper, S., Corley, A., 2019. Acceleration of ice loss across the Himalayas over the past 40 years. Sci. Adv. 5 (6), eaav7266. https://doi.org/10.1126/sciadv.aav7266.

Mishra, B., Babel, M.S., Tripathi, N.K., 2014. Analysis of climatic variability and snow cover in the Kaligandaki river basin, Himalaya, Nepal. Theor. Appl. Climatol. 116 (3–4), 681–694. https://doi.org/10.1007/s00704-013-0966-1.

Mishra, A.K., 2019. Quantifying the impact of global warming on precipitation patterns in India. Meteorol. Appl. 26 (1), 153–160.

Mishra, A., Rafiq, M., 2017. Towards combining GPM and MFG observations to monitor near real time heavy precipitation at fine scale over India and nearby oceanic regions. Dynam. Atmos. Oceans 80, 62–74.

Mishra, A.K., Nagaraju, V., Rafiq, M., Chandra, S., 2019. Evidence of links between regional climate change and precipitation extremes over India. Weather 74 (6), 218–221.

Mountain Research Initiative EDW Working Group, 2015. Elevation-dependent warming in mountain regions of the world. Nat. Clim. Change 5 (5), 424–430. https://doi.org/10.1038/nclimate2563.

O'Callaghan, J.F., Mark, D.M., 1984. The extraction of drainage networks from digital elevation data. Comput. Vis. Graph Image Process 28 (3), 323–344. https://doi.org/10.1016/S0734-189X(84)80011-0.

Peng, M., Wang, X., Zhang, G., Veh, G., Sattar, A., Chen, W., Allen, S., 2023. Cascading hazards from two recent glacial lake outburst floods in the Nyainqêntanglha range, Tibetan Plateau. J. Hydrol. 626, 130155. https://doi.org/10.1016/j.jhydrol.2023.130155.

Pronk, J.B., Bolch, T., King, O., Wouters, B., Benn, D.I., 2021. *Proglacial lakes elevate glacier surface Velocities in the Himalayan region* (preprint). Glaciers/Rem. Sens. https://doi.org/10.5194/tc-2021-90.

Rafiq, M., Mishra, A.K., 2018. A study of heavy snowfall in Kashmir, India in January 2017. Weather 73 (1), 15–17.

Rafiq, M., Romshoo, S.A., Mishra, A.K., Jalal, F., 2019. Modelling Chorabari Lake outburst flood, Kedarnath, India. J. Mt. Sci. 16 (1), 64–76. https://doi.org/10.1007/s11629-018-4972-8.

RGI Consortium, 2023. Randolph Glacier inventory - a dataset of global glacier outlines. NASA National Snow and Ice Data Center Distributed Active Archive Center. https://doi.org/10.5067/F6JMOVY5NAVZ. [Data set], Version 7.

Rinzin, S., Zhang, G., Sattar, A., Wangchuk, S., Allen, S.K., Dunning, S., Peng, M., 2023. GLOF hazard, exposure, vulnerability, and risk assessment of potentially dangerous glacial lakes in the Bhutan Himalaya. J. Hydrol. 619, 129311. https://doi.org/10.1016/j.jhydrol.2023.129311.

Romshoo, S.A., Rafiq, M., Rashid, I., 2018. Spatio-temporal variation of land surface temperature and temperature lapse rate over mountainous Kashmir Himalaya. J. Mt. Sci. 15 (3), 563–576. https://doi.org/10.1007/s11629-017-4566-x.

Sattar, A., Goswami, A., Kulkarni, A.V., 2019. Hydrodynamic moraine-breach modeling and outburst flood routing - a hazard assessment of the South Lhonak lake, Sikkim. Sci. Total Environ. 668, 362–378. https://doi.org/10.1016/j.scitotenv.2019.02.388.

Sattar, A., Goswami, A., Kulkarni, Anil V., Emmer, A., Haritashya, U.K., Allen, S., et al., 2021. Future Glacial Lake Outburst flood (GLOF) hazard of the SouthSouth Lhonak lake, Sikkim Himalaya. Geomorphology 388, 107783. https://doi.org/10.1016/j.geomorph.2021.107783.

Save, H., Bettadpur, S., Tapley, B.D., 2016. High-resolution CSR GRACE RL05 mascons. J. Geophys. Res. Solid Earth (121), 7547–7569. https://doi.org/10.1002/2016JB013007. Received.

Sharma, R.K., Pradhan, P., Sharma, N.P., Shrestha, D.G., 2018. Remote sensing and in situ-based assessment of rapidly growing South Lhonak glacial lake in eastern Himalaya, India. Nat. Hazards 93 (1), 393–409. https://doi.org/10.1007/s11069-018-3305-0.

Shugar, D.H., Jacquemart, M., Shean, D., Bhushan, S., Upadhyay, K., Sattar, A., et al., 2021. A massive rock and ice avalanche caused the 2021 disaster at Chamoli, Indian Himalaya. Science 373 (6552), 300–306. https://doi.org/10.1126/science.abh4455.

Shugar, Dan H., Burr, A., Haritashya, U.K., Kargel, J.S., Watson, C.S., Kennedy, M.C., et al., 2020. Rapid worldwide growth of glacial lakes since 1990. Nat. Clim.

Change 10 (10), 939–945. https://doi.org/10.1038/s41558-020-0855-4.
Shukla, A., Garg, P.K., Srivastava, S., 2018. Evolution of glacial and high-altitude lakes in the Sikkim, eastern Himalaya over the past four decades (1975–2017). Front. Environ. Sci. 6, 81. https://doi.org/10.3389/fenvs.2018.00081.
Song, C., Sheng, Y., Wang, J., Ke, L., Madson, A., Nie, Y., 2017. Heterogeneous glacial lake changes and links of lake expansions to the rapid thinning of adjacent glacier termini in the Himalayas. Geomorphology 280, 30–38. https://doi.org/10.1016/j.geomorph.2016.12.002.
Taylor, C., Robinson, T.R., Dunning, S., Rachel Carr, J., Westoby, M., 2023. Glacial lake outburst floods threaten millions globally. Nat. Commun. 14 (1), 487. https://doi.org/10.1038/s41467-023-36033-x.
Thakuri, S., Salerno, F., Bolch, T., Guyennon, N., Tartari, G., 2016. Factors controlling the accelerated expansion of Imja lake, mount everest region, Nepal. Ann. Glaciol. 57 (71), 245–257. https://doi.org/10.3189/2016AoG71A063.
Veh, G., Korup, O., Von Specht, S., Roessner, S., Walz, A., 2019. Unchanged frequency of moraine-dammed glacial lake outburst floods in the Himalaya. Nat. Clim. Change 9 (5), 379–383. https://doi.org/10.1038/s41558-019-0437-5.
Veh, G., Korup, O., Walz, A., 2020a. Hazard from Himalayan glacier lake outburst floods. Proc. Natl. Acad. Sci. USA 117 (2), 907–912. https://doi.org/10.1073/pnas.1914898117.
Veh, G., Korup, O., Walz, A., 2020b. Hazard from Himalayan glacier lake outburst floods. Proc. Natl. Acad. Sci. USA 117 (2), 907–912. https://doi.org/10.1073/pnas.1914898117.
Wang, J., Chen, F., Zhang, M., Yu, B., 2022. NAU-net: a new deep learning framework in Glacial Lake detection. Geosci. Rem. Sens. Lett. IEEE 19, 1–5. https://doi.org/10.1109/LGRS.2022.3165045.
Wang, S., Peppa, M.V., Xiao, W., Maharjan, S.B., Joshi, S.P., Mills, J.P., 2022. A second-order attention network for glacial lake segmentation from remotely sensed imagery. ISPRS J. Photogrammetry Remote Sens. 189, 289–301. https://doi.org/10.1016/j.isprsjprs.2022.05.007.
Wang, W., Zhang, T., Yao, T., An, B., 2022. Monitoring and early warning system of Cirenmaco glacial lake in the central Himalayas. Int. J. Disaster Risk Reduc. 73, 102914. https://doi.org/10.1016/j.ijdrr.2022.102914.
Wang, Xin, Guo, X., Yang, C., Liu, Q., Wei, J., Zhang, Y., et al., 2020. Glacial lake inventory of high-mountain Asia in 1990 and 2018 derived from Landsat images. Earth Syst. Sci. Data 12 (3), 2169–2182. https://doi.org/10.5194/essd-12-2169-2020.
Wang, Xue, Zhang, G., Veh, G., Sattar, A., Wang, W., Allen, S.K., et al., 2024. Reconstructing glacial lake outburst floods in the Poiqu River basin, central Himalaya. Geomorphology 449, 109063. https://doi.org/10.1016/j.geomorph.2024.109063.
Worni, R., Huggel, C., Stoffel, M., 2013. Glacial lakes in the Indian Himalayas — from an area-wide glacial lake inventory to on-site and modeling based risk assessment of critical glacial lakes. Sci. Total Environ. 468–469, S71–S84. https://doi.org/10.1016/j.scitotenv.2012.11.043.
Zhang, G., Bolch, T., Yao, T., Rounce, D.R., Chen, W., Veh, G., et al., 2023. Underestimated mass loss from lake-terminating glaciers in the greater Himalaya. Nat. Geosci. 16 (4), 333–338. https://doi.org/10.1038/s41561-023-01150-1.
Zhang, T., Wang, W., Gao, T., An, B., Yao, T., 2022. An integrative method for identifying potentially dangerous glacial lakes in the Himalayas. Sci. Total Environ. 806, 150442. https://doi.org/10.1016/j.scitotenv.2021.150442.
Zhang, T., Wang, W., An, B., Wei, L., 2023. Enhanced glacial lake activity threatens numerous communities and infrastructure in the Third Pole. Nat. Commun. 14 (1), 8250. https://doi.org/10.1038/s41467-023-44123-z.
Zheng, G., Allen, S.K., Bao, A., Ballesteros-Cánovas, J.A., Huss, M., Zhang, G., et al., 2021. Increasing risk of glacial lake outburst floods from future Third Pole deglaciation. Nat. Clim. Change 11 (5), 411–417. https://doi.org/10.1038/s41558-021-01028-3.